



Styrene alters potassium endolymphatic concentration in a model of cultured utricle explants



V. Tallandier^{a,b}, L. Merlen^a, S. Boucard^a, A. Thomas^a, T. Venet^{a,b}, M. Chalansonnet^{a,*}, G. Gauchard^b, P. Campo^{a,b}, B. Pouyatos^a

^a Institut National de Recherche et de Sécurité, Rue du Morvan, CS 60027, F-54519 Vandœuvre, Cedex, France

^b DevAH EA 3450 – Développement, Adaptation et Handicap, Régulations cardio-respiratoires et de la motricité-Université de Lorraine, F-54500 Vandœuvre, France

ARTICLE INFO

Keywords:

Styrene
Vestibular explants
Potassium
Endolymph
Rat
Organotypic culture

ABSTRACT

Despite well-documented neurotoxic and ototoxic properties, styrene remains commonly used in industry. Its effects on the cochlea have been extensively studied in animals, and epidemiological and animal evidence indicates an impact on balance. However, its influence on the peripheral vestibular receptor has yet to be investigated. Here, we assessed the vestibulotoxicity of styrene using an *in vitro* model, consisting of three-dimensional cultured newborn rat utricles filled with a high-potassium (K^+) endolymph-like fluid, called “cysts”. K^+ entry in the cyst (“influx”) and its exit (“efflux”) are controlled by secretory cells and hair cells, respectively. The vestibular epithelium’s functionality is thus linked to K^+ concentration, measured using a microelectrode.

Known inhibitors of K^+ efflux and influx validated the model. Cysts were subsequently exposed to styrene (0.25; 0.5; 0.75 and 1 mM) for 2 h or 72 h. The decrease in K^+ concentration measured after both exposure durations was dose-dependent, and significant from 0.75 mM styrene. Vacuoles were visible in the cytoplasm of epithelial cells from 0.5 mM after 2 h and from 0.25 mM after 72 h.

The results presented here are the first evidence that styrene may deregulate K^+ homeostasis in the endolymphatic space, thereby altering the functionality of the vestibular receptor.

1. Introduction

Aromatic solvents have many applications in industry, and long-term exposure to some of them has been shown to impair vigilance and postural stability (Vouriot et al., 2005). Consequently, exposure to solvents may increase the risks of occupational accidents and affect the quality of life of workers. Styrene is one of the most extensively used industrial solvents, mainly as a precursor of polymers and copolymers. Styrene is used in boat, automobile, aircrafts construction and their highest potential exposure to this chemical is reported in occupational setting for the production of glass-reinforced plastics (Miller et al., 1994). In addition to neurotoxic effects described in humans (Bergamaschi et al., 1997; Kishi et al., 2000), several animal and epidemiological studies indicate that styrene has deleterious effects on hearing (Hoet and Lison, 2008; Johnson, 2007; Loquet et al., 1999; Pleban et al., 2017) and balance (Calabrese et al., 1996; Larsby et al., 1978; Möller et al., 1990; Niklasson et al., 1993; Toppila et al., 2006).

These studies show that styrene may cause elevation of the auditory threshold and alter postural performances and vestibular reflexes. Most of the reports relating to styrene-induced balance impairments assumed the vestibular system to be affected. However, no clear demonstration of the precise mechanism – whether through an effect on the peripheral end-organ or an impact on central structures and pathways – has yet been provided (for review, see Gans et al., 2019).

In contrast, the effect of styrene on the cochlea is well described: electrophysiological measurements in rats exposed to styrene vapors showed an auditory deficit related to dose-dependent loss of cochlear outer hair cells (OHC) (Lataye et al., 2001). An *in vivo* study comparing level of OHC losses of 21 aromatic solvents showed that styrene is one of the most ototoxic agents among these tested chemicals (Gagnaire and Langlais, 2005). Because of its high lipophilicity styrene is assumed to reach the OHCs through the membranes of the cells constituting the outer sulcus within the organ of Corti, and not through the liquids contained in the inner ear. Campo et al. (1999) suggested that styrene

Abbreviations: 3D, three-dimensional; DC, Dark Cells; DIV, Days *in vitro*; DMEM-F12, Dulbecco’s Modified Eagle Medium / Nutrient Mixture F-12; HC, Hair Cells; K^+ , Potassium ion; MET, mechano-electrical transduction; Na/K-ATPase, Sodium-Potassium Adenosine Triphosphate pump; NKCC1, Na-K-Cl co-transporter 1; OHC, Outer Hair Cells; P, Post-natal day; PBS, Phosphate-Buffered Saline; TC, Transitional Cells

* Corresponding author.

E-mail address: monique.chalansonnet@inrs.fr (M. Chalansonnet).

<https://doi.org/10.1016/j.tiv.2020.104915>

Received 27 January 2020; Received in revised form 2 June 2020; Accepted 11 June 2020

Available online 12 June 2020

0887-2333/ © 2020 Elsevier Ltd. All rights reserved.

reaches the cochlea through the stria vascularis, from where it can access the organ of Corti and thus the OHCs. Several authors have shown that Deiters' cells may be damaged by solvents at doses that do not induce OHC loss (Campo et al., 2001; Chen et al., 2007; Fetoni et al., 2016). Since Deiters' cells are involved in K^+ re-uptake from OHCs (Hibino and Kurachi, 2006; Spicer and Schulte, 1998), some authors have suggested that styrene exposure affects the K^+ cycle (Campo et al., 2001; Fetoni et al., 2016). Although this hypothesis has never been experimentally confirmed, it is reasonable to assume that ototoxicity is not limited to disruption of the OHC, but also perturbs ionic balance in inner ear fluids.

To our knowledge, no study has yet demonstrated the impact of an aromatic solvent, such as styrene, on the vestibular receptor. Both auditory and vestibular receptors are composed of sensory hair cells and secretory cells – stria marginal cells and vestibular dark cells – involved in inner ear fluid homeostasis. Moreover, cochlear and vestibular endolymph both exhibit a high K^+ concentration required to permit mechano-electrical transduction (MET) at the level of the sensory hair cells (Ciuman, 2009; Hibino et al., 2010). Given these similarities, in addition to its cochleotoxic effect, we hypothesize that styrene may be vestibulotoxic. In support of this hypothesis, other ototoxic agents – such as cisplatin, gentamicin, or nitriles – have been linked to balance disorders related to disruption of the neurosensory epithelium within the vestibular receptor (Callejo et al., 2017; Kim et al., 2013; Llorens et al., 1993).

Given the number of unknowns surrounding the vestibulotoxic properties of aromatic solvents and the time-consuming *in vivo* studies that would be needed to investigate the ototoxic mechanisms of these chemicals, a fast and reliable *in vitro* method is required to assess the functional and histological consequences of solvent exposure on the vestibular end-organ.

Here, we used newborn rat utricles cultured in three-dimensional (3D) medium as a model to assess the potency vestibulotoxic of styrene (Bartolami et al., 2011; Gaboyard et al., 2005). This *in vitro* model, initially developed to investigate endolymph formation in immature vestibule consists in a sphere, called “cyst”, which forms when the harvested utricle is placed in the 3D medium. After a few days in culture, the volume of the cyst increases as it fills with an endolymph-like fluid. All utricular cell types (hair cells, transitional and dark cells) and their associated proteins involved in K^+ cycling (MET channels, Na/K-ATPase and Na-K-2Cl co-transporter 1 (NKCC1)) are preserved in the “cysts” and contribute to endolymph production (Bartolami et al., 2011; Gaboyard et al., 2005). Acquisition of hair cells sensory transduction at embryonic state (Géléoc and Holt, 2003) and complete maturation of vestibular dark cells observed around the 4th day post-partum (Anniko and Nordemar, 1980), are in line with the production of an endolymph-like fluid in the lumen of the cyst.

The biochemical composition of endolymph therefore depends on the functionality of utricular cells. For this study, the potential vestibulotoxicity of styrene was investigated by measuring its effect on the endolymphatic K^+ concentration using an electrochemical method, and by observing its histopathological consequences on the vestibular sensory epithelium.

2. Materials and methods

2.1. Animals

Pregnant Long-Evans female rats were purchased from Janvier Laboratories and were housed in individual cages (surface: 1032 cm²; height: 20 cm) from the 15th day of pregnancy until birth under a 12 h light / 12 h dark cycle. In the animal facilities, temperature was maintained at 22 ± 2 °C and relative humidity at 55 ± 15%. Food and water were available *ad libitum*. Animals were weighed upon arrival at the facility and just before giving birth to monitor weight gain during the third week of pregnancy. Birth was natural, and newborns

aged between 0 (P0) and 4 post-natal days (P4) were used in experiments. All investigations involving animals were performed in accordance with the Guide for Care and Use of Laboratory Animals promulgated by the European parliament and council (EUROPEAN DIRECTIVE 2010/63/EU, 22 September 2010). The animal facilities are accredited by the French Ministry of Agriculture (Authorization N° D 54–547-10).

2.2. Three-dimensional culture of utricle explants

The utricle explants were cultured using a technique described in previous studies (Bartolami et al., 2011; Gaboyard et al., 2005). Newborn rats (P0-P4) were decapitated and the head was hemisectioned. The temporal bones were harvested and placed in Leibovitz's L-15 medium. Utricles were aseptically removed, taking care to conserve the epithelium covering the macula. The basal surface of the sensory epithelium was stripped of surrounding nervous tissue. Explants were then placed on 12-mm diameter glass coverslips previously coated with 10 µg/ml laminin (Sigma-Aldrich, Saint-Louis, MO, U.S.A.) in 35-mm Petri dishes. Ten microliters of Matrigel® (Corning, NY, USA) was gently overlaid on the vestibular structures. To allow explants to grow, they were positioned so that the basal surface of the sensory epithelium faced the coverslips. Cultures were incubated at 37 °C for 30 min in a 95% O₂ / 5% CO₂ atmosphere in a humidified incubator. Embedded utricular explants were then covered with culture medium Dulbecco's Modified Eagle Medium / Nutrient Mixture F-12 (DMEM-F12, Thermo Fisher Scientific, Waltham, MA, USA) supplemented with 2% N-2 (Life Technologies, Carlsbad, California). Vestibular explants were maintained at 37 °C in a humidified 5% CO₂ atmosphere and half of the culture medium was renewed three times per week. After a few days *in vitro* (DIV), the utricular structures sealed themselves and formed a vesicle enclosing the endolymphatic compartment (“cyst”). Deflated cysts were excluded from the study.

2.3. Electrophysiological measurements

The potassium concentration inside the vesicle was determined using an ion-sensitive microelectrode. Borosilicate glass capillaries with filament (1B100F-4; WPI, Sarasota, FL, USA) were melted and pulled vertically using a PUL-100 Microprocessor-controlled micropipette Puller (WPI, Sarasota, FL, USA) before baking at 200 °C for 2 h to eliminate proteins contaminant among others. Microelectrodes were then silanized with dichlorodimethylsilane (Sigma-Aldrich, Saint-Quentin Fallavier, France) vapors for 5 min to create a hydrophobic layer inside the microelectrode. Capillaries were dried by baking for 4 h at 200 °C. The microelectrode tip was backfilled with liquid membrane ion K^+ exchanger (Potassium Ionophore I – Cocktail B, Sigma-Aldrich, Saint-Quentin Fallavier, France) and the barrel was filled with 150 mM KCl. Microelectrode impedance was determined using an ohmmeter (Omega TipZ, WPI, Sarasota, USA) to select microelectrodes with an impedance of less than 200 MΩ. Microelectrodes were connected, *via* a holder, to the headstage amplifier of a differential electrometer (HiZ-223 Warner Instruments, Hamden, USA). The reference electrode was immersed in the calibration solutions or the medium covering the sample to close the electrical circuit. The electrical signal was monitored with Pulse® software and a 3160-A-022 analyzer (Brüel & Kjær, Nærum, Denmark). Before recording the electrical potential of the cyst's endolymphatic compartment, the electrical signal of the microelectrode was calibrated with decreasing concentration of KCl solutions: 150, 100, 75, 50, 20 and 10 mM. All calibration solutions contained 150 mM cation, supplemented with NaCl as appropriate.

To measure the K^+ concentration in the endolymphatic compartment, cysts were placed on the microscope stage and covered with medium. Before measuring the potassium concentration of the endolymphatic compartment, the microelectrode tip was immersed in the medium, which contained a known K^+ concentration (about 4 mM KCl,

DMEM-F12, Thermo Fisher Scientific). Then, the ion-sensitive micro-electrode was inserted into the vesicle explants under optical control. Once inside the vesicle, the stabilization of the signal took few second and the duration of the K^+ measurement never exceeded 30 s.

2.4. Pharmacological treatment

Several pharmacological molecules known to alter the activity of ion channels and pumps were added to the culture medium to test their effects on the endolymphatic K^+ concentration. Ouabain (a Na/K-ATPase inhibitor), bumetanide (a NKCC1 inhibitor disrupting potassium entry in the cyst), gentamicin and gadolinium (which both block mechano-electrical transduction channels at the top of stereocilia of hair cells), were tested in the present study. Ouabain, gadolinium chloride hexahydrate, gentamicin solution and bumetanide were purchased from Sigma-Aldrich (Saint-Quentin Fallavier, France). At 7 DIV, cysts were incubated with gentamicin (1 mM, 2 h), gadolinium (0.1 mM, 2 h), ouabain (1 mM, 2 h) or bumetanide (0.05 mM, 0.5 h), and the effects of these pharmacological treatments were measured. In parallel, control cultures were incubated in the same conditions with the corresponding vehicle.

2.5. Styrene exposure

Styrene (Acros Organics, Illkirch, France; 99%) was added directly to DMEM-F12 medium (Thermo Fisher Scientific, Waltham, MA, USA) in a volumetric flask to prepare the different stock solutions of styrene: 0.25, 0.5, 0.75 and 1 mM. The styrene-medium solution and 2% N-2 were added to glass headspace vials (8 ml) which were then sealed with a Teflon-faced butyl rubber septum and an aluminum crimp cap to avoid solvent evaporation. Each vial was completely filled in order to have no gaseous phase, thus avoiding styrene stagnation in this compartment. The vial caps were removed to place cysts in contact with medium containing styrene before sealing once again. Cysts were maintained in these conditions for 2 h or 72 h, to observe acute and cytotoxic effects of styrene respectively, prior to measuring the K^+ concentration at 7 DIV. For 2-h exposures, the treatment was performed at 7 DIV, whereas for 72-h exposures, cysts were maintained in culture with styrene from the 4th DIV to the 7th DIV. Control cysts were cultivated in medium without styrene in the same sealed chemical vials for 2 h or 72 h.

2.6. Tissue section preparation for light microscopy

After culturing for 7 DIV, cysts were collected and fixed with 2.5% glutaraldehyde in 0.2 M cacodylate buffer for 24 h. Samples were rinsed in 0.2 M cacodylate buffer and post-fixed for 1 h with 1% osmium tetroxide in the dark. Cysts were dehydrated in graded ethanol concentrations up to 100% and then embedded in epoxy resin after soaking in incremental 50%/50% and 75%/25% resin / propylene oxide solutions. Following polymerization at 60 °C for 24 h, 2.5- μ m transversal sections were cut with a microtome (Leica, UC7), and stained with toluidine blue (Sigma-Aldrich, Saint-Quentin Fallavier, France). Sections were observed with an optical microscope (BX41, Olympus, Tokyo, Japan).

2.7. Immunohistochemical analysis of cleaved caspase-3

The embedded Matrigel® was removed and cysts were fixed with 4% formaldehyde buffered at pH 6.9 for 24 h. After rinsing with Phosphate-Buffered Saline (PBS), cysts were dehydrated in graded ethanol concentrations up to 100%. After a clearing step in xylene, samples were embedded in paraffin. Transversal sections (4 μ m) were cut with a microtome (Microm, HM 340E). Slices were dewaxed in xylene and rehydrated. A heat-induced antigen retrieval step was performed in citrate buffer (10 mM, pH 6) for 5 min. To reduce nonspecific staining,

endogenous peroxidase activity was blocked with 3% H_2O_2 for 5 min, and nonspecific antibody binding sites were blocked with 5% of normal goat serum for 1 h at room temperature. Sections were incubated with the cleaved anti-caspase 3 monoclonal rabbit antibody (dilution 1/800, Cell Signaling, MA, USA) overnight at 4 °C. After rinsing in TBST-1 \times , sections were incubated with the detection reagent containing peroxidase enzyme (SignalStain® Boost Detection Reagent, Cell Signaling) for 30 min at room temperature. The immunoreaction was visualized with 3,3'-diaminobenzidine (DAB), and sections were counterstained with Mayer Haemalum. Sections were mounted and observed under the optical microscope.

2.8. Statistical analysis

Results were expressed as mean \pm standard error of the mean (SEM). The difference between experimental groups was determined using one-way ANOVA. Statistical results were expressed as follows: F (dfb, dfr) = F-ratio; $p = p$ value, where dfb is the number of degrees of freedom between groups, and dfr is the number of residual degrees of freedom. A post-hoc least-significant difference test (LSD) was run to compare variations between "DIV" groups, and Dunnett's method was used to compare variations between control and the various styrene concentration groups. Student's *t*-test was applied to compare two experimental conditions. The threshold for statistical significance was set at $p = .05$.

3. Results

3.1. Endolymphatic compartment development in utricle explants

Utricles were dissected from P2 rats, and the morphological development of utricle explants was monitored from the day the tissue was placed in culture (0 DIV) until the 7th DIV (Fig. 1.A). After 1 DIV in the extracellular matrix, the utricle explants were surrounded by growing fusiform cells, possibly fibroblasts. At 2 DIV, the utricle explants appeared swollen and a small vesicle was observable. At 5 DIV, the vesicles had reached their maximum size, which remained unchanged until 7 DIV.

The endolymphatic K^+ concentration was monitored from 2 to 9 DIV (Fig. 1.B). A progressive accumulation of K^+ was measured between 2 DIV (39.6 ± 4.0 mM) and 4 DIV (83.1 ± 5.2 mM), at which time it reached a plateau which was maintained until 7 DIV (85.8 ± 4.8 mM). These differences in K^+ concentration were significant [F = (7, 79) = 10.33; $p < .001$]. Post-hoc comparisons between groups show that the K^+ concentrations measured at 2 and 3 DIV were significantly lower ($p < .05$) than those measured between 4 and 9 DIV. Potassium concentrations were not significantly different between 4 and 9 DIV ($p > .05$).

The endolymphatic K^+ concentration was measured in 7-DIV cysts obtained from newborn rat utricles harvested at different postnatal days (Fig. 1.C). The one-way ANOVA does not reveal any difference between groups [F (4, 96) = 1.13; $p = 0.346$], indicating that culture development is not dependent on the day of utricle was dissected.

3.2. Effects of K^+ "influx" or "efflux" inhibitors on endolymphatic concentration

Secretory cells (transitional and dark cells) are responsible of the K^+ "influx", the term "influx" being defined as the passage of K^+ ions from the culture medium to the endolymphatic space (Fig. 2). Na/K-ATPase and NKCC1 expressed at their basolateral pole control the K^+ uptake (Bartolami et al., 2011). Potassium ions are released in endolymphatic compartment though the complex KCNQ1/KCNE1 expressed at the apical side of dark cells and the two-pore-domain K^+ channels (K_{2p}) expressed in the apical membrane of dark and transitional cells (Nicolas et al., 2001, 2004; Popper et al., 2008). Conversely, K^+ "efflux", i.e. the

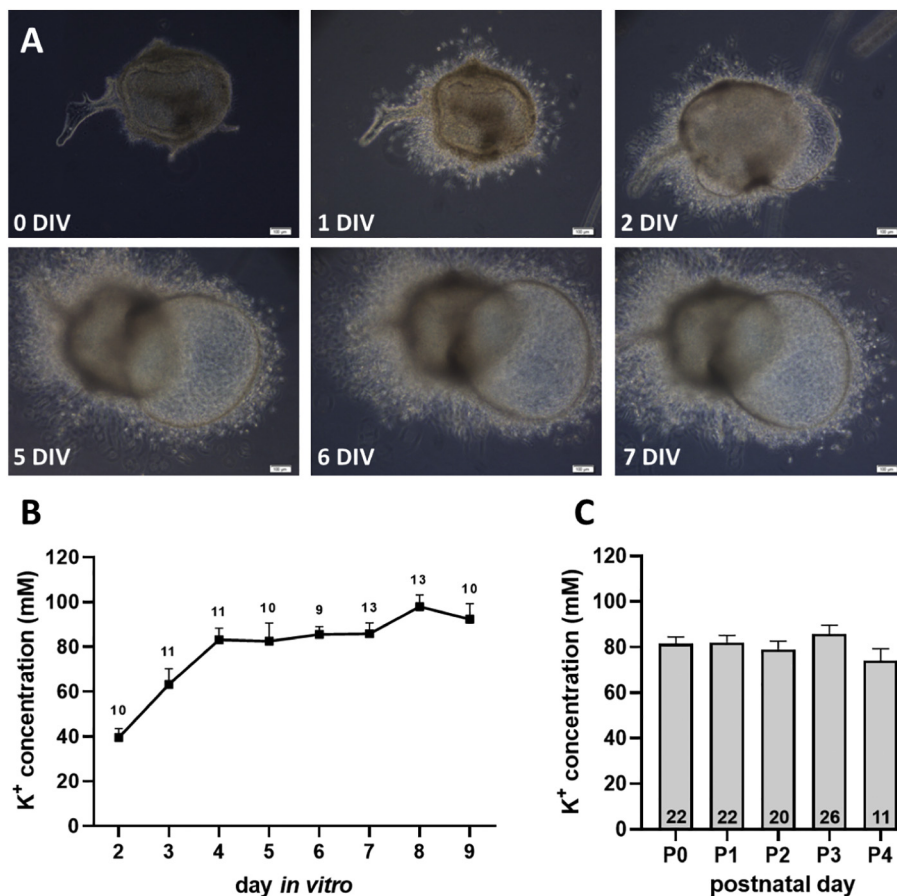


Fig. 1. Morphological and functional developments of 3D utricle explants. (A) Newborn rat utricles were dissected at post-natal day 2 (P2) and maintained for 7 days *in vitro* (DIV). Light microscopy pictures show morphological evolution and cyst formation of cultured utricles from 0 to 7 DIV. Scale bar = 100 μ m. (B) Endolymphatic potassium accumulation in cysts from P0-P4 newborn rats was measured from 2 to 9 DIV. (C) Endolymphatic K⁺ concentration of 7-DIV cysts obtained from newborn rat utricles was measured as function of postnatal day. Mean \pm SEM; the number of samples are indicated above each symbol (B) or in each bar of the histogram (C).

movement of the K⁺ ions from the endolymphatic space to the culture medium, is performed by sensory hair cells involved in mechano-electrical transduction. Endolymphatic K⁺ enters the hair cells through the MET channels, a phenomenon which depolarizes the cells and results in the excitation of the afferent neurons. Recovery of the resting membrane potential is then dependent on the K⁺ exit across the basolateral membrane of the hair cells mainly through voltage-gated K⁺ channels, whose molecular identity remains unclear (Meredith and Rennie, 2016).

Fig. 3 shows that gentamicin and gadolinium, both of which reversibly block the MET channels in hair cell's stereocilia, significantly increased the K⁺ concentration in 7 DIV cysts. K⁺ concentration was increased by 14% after exposure to gentamicin (treated group: 100.75 \pm 3.2 mM vs. control group: 88.2 \pm 3.3 mM; $p = .028$) and by 20% upon incubation with gadolinium (treated group: 103.9 \pm 5.1 mM vs. control group: 86.8 \pm 4.7 mM; $p = .028$). Conversely, ouabain and bumetanide significantly decreased the K⁺ concentration: ouabain treatment (1 mM, 2 h) caused a drastic 65% reduction in K⁺ (treated group: 29.8 \pm 5.5 mM vs. control group: 84.4 \pm 5.7 mM; $p < .001$), whereas bumetanide (0.05 mM, 0.5 h) triggered a 22% decrease in K⁺ concentration in 7 DIV cysts (treated group: 61.2 \pm 6.3 mM vs. control group: 78.7 \pm 2.82 mM; $p = .014$). A one-way ANOVA comparing the different control groups showed no significant difference [$F(3, 49) = 1.06$; $p = .373$].

3.3. Effect of styrene on endolymphatic K⁺ concentration

Cysts were maintained in contact with varying styrene concentrations (0.25; 0.5; 0.75 and 1 mM) for either 2 or 72 h (Fig. 4A,B). For the 72-h condition, utricle explants were treated from the 4th DIV to 7th DIV, when the K⁺ concentration is the most stable (Fig. 1B).

Exposure to styrene for 2 or 72 h caused dose-dependent decreases

in K⁺ concentrations [2 h: $F(4, 38) = 8.43$; $p = .0001$ –72 h: $F(4, 54) = 17.99$; $p < .0001$].

After exposure to styrene for 2 h, K⁺ concentration decreased significantly compared to control group (82.0 \pm 4.8 mM) for cysts exposed to 0.75 mM (53.2 \pm 7.0 mM; $p = .014$) and 1 mM styrene (41.7 \pm 11.6 mM; $p < .001$). The decline in concentration was 35.12% and 49.13%, respectively. Exposure for 72 h also triggered a significant decrease in K⁺ concentration compared to the control group (80.6 \pm 4.5 mM) in the 0.75 mM (59.1 \pm 4.9 mM; $p = .004$) and 1 mM (21.0 \pm 5.9 mM; $p < .001$) groups. The reductions measured were 22.75% and 73.97%, respectively.

3.4. Histological analysis

To determine if styrene induced an apoptotic pathway mechanism, cleaved caspase-3 was immuno-stained. Antibody-staining revealed no caspase-3 activation in cysts exposed to styrene for 72 h, whatever the concentration assessed (data not shown).

The gross morphologies of epithelial cells (P1–4, 7 DIV) in cysts exposed to styrene (0; 0.25; 0.5; 0.75 and 1 mM) for 2 or 72 h were observed under light microscopy (Figs. 5 and 6). In control samples, type I (pyriform shape) and type II (column-shaped) hair cells and intercalated supporting cells could be clearly distinguished in the sensory epithelium. No obvious morphological alterations to epithelial cells were observed, with no vacuoles visible in the cytoplasm, and normal-looking nuclei. A layer of secretory cells bordering the sensory epithelium was identifiable. It consisted of cuboidal dark cells and transitional cells, the latter of which are in contact with sensory cells. Cysts exposed to 1 mM of styrene for 2 h or 72 h contained cells with condensed and/or swollen nuclei, low-density cytoplasm, and displayed vacuolization. This effect was visible in all cell types in the sensory and secretory epithelia. Some hair cells were extruded from the cuticular plate, but

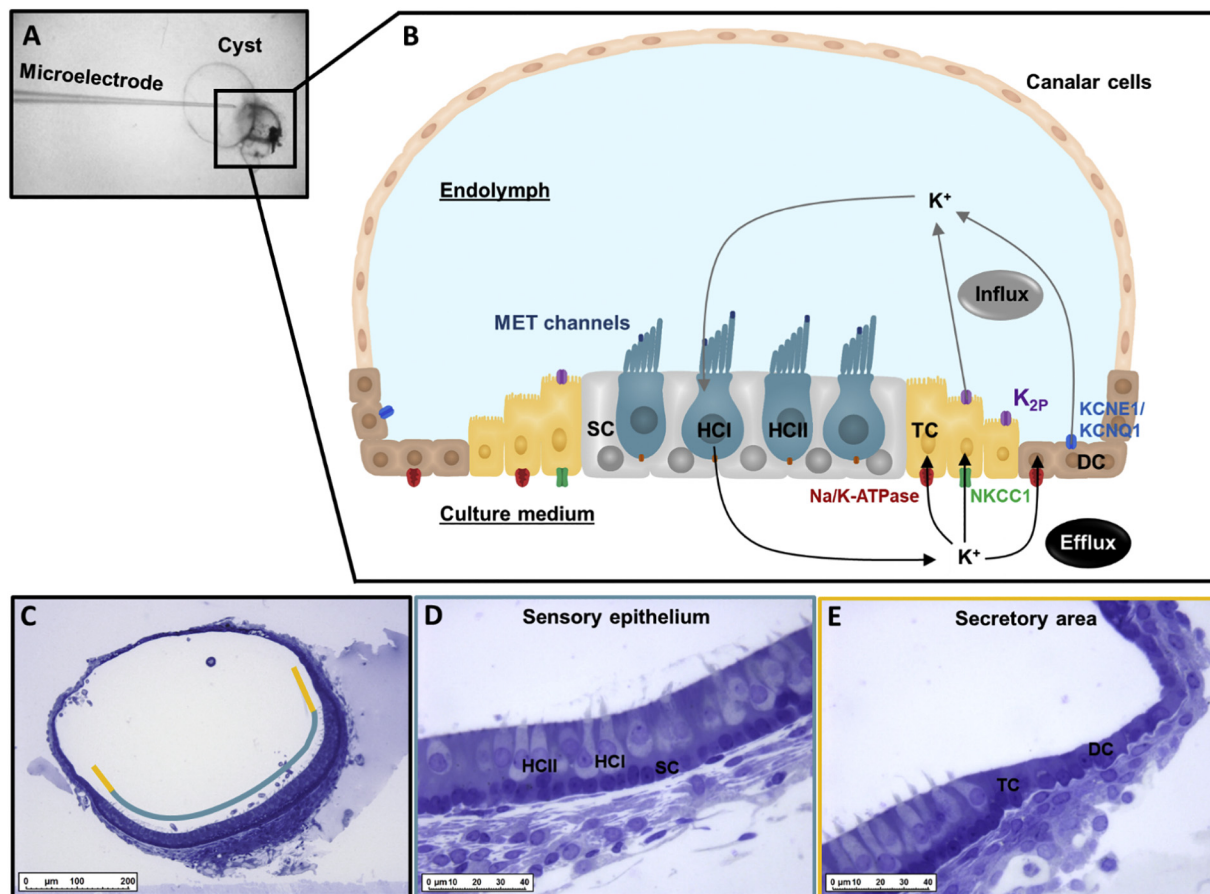


Fig. 2. Description of the 7 DIV cyst: (A) Photograph an ion-sensitive microelectrode penetrating a cyst during the recording of the K^+ concentration. (B) Schematic representation of a 7-DIV cyst. The cyst is an enclosed structure filled with a high- K^+ endolymph-like fluid, which contains sensory and secretory cells participating in the K^+ cycle. Transitional cells (TC) and dark cells (DC) are involved in K^+ “influx”, i.e. the passage of K^+ ions from the culture medium to the endolymphatic compartment. These cells absorb K^+ ions from the culture medium via Na/K-ATPase and NKCC1 channels expressed at their basolateral membrane and release them in the endolymphatic compartment at their apical side through KCNE1/KCNQ1 and K_{2P} channels. K^+ “efflux”, i.e. the movement of K^+ ions from the endolymphatic compartment to the culture medium is ensured by sensory hair cells. Mechano-electrical transducer (MET) channels expressed in the hair cell stereocilia allow the passage of K^+ ions into the cytosol, which in turn triggers depolarization and the release of K^+ ions in the culture medium through voltage-gated K^+ channels expressed in basolateral membrane (C) Semi-thin sections of 7-DIV obtained from P2 newborn rat utricle were observed in light microscopy. The sensory epithelium is indicated in green and secretory area in yellow. (D) The sensory epithelium is composed of supporting cells (SC) and 2 types of hair cells expressed ciliary bundles at their apical surface; pyriform-shaped type I hair cell (HCI) and column-shaped type II hair cell (HCII). (E) The secretory area is composed of transitional cells (TC) neighbored cubic-shaped dark cells (DC). Scale bar = 200 μm in C and 40 μm in D, E. (For interpretation of the references to colour in this figure legend, the reader is referred to the web version of this article.)

most stereocilia remained present. Small numbers of vacuoles were visible in epithelial cells of cysts exposed to 0.5 and 0.75 mM of styrene for 2 h, whereas no sign of cellular damage was observed in cysts exposed to 0.25 mM styrene. After 72 h exposure, cytoplasmic vacuoles were observed in all epithelial cell types in cysts exposed to styrene at a concentration exceeding 0.25 mM. Apart from cytoplasmic vacuoles observed in the various sensory and secretory epithelial cells in cysts, no other obvious features of cell injury were noted.

4. Discussion

For this study, the adverse effects of styrene on the vestibular receptor were investigated using an *in vitro* model adapted from Bartolami et al., (2011) and Gaboyard et al., (2005). This model consisted in a 3D utricular explant from newborn rats, and was compatible with the assessment of both functional and morphological consequences of styrene exposure on utricular cells.

Morphological changes and electrophysiological recordings over time demonstrated a progressive maturation of this model (Fig. 1). After two days in culture, the 3D utricular explant displayed a small vesicle. We assumed that epithelial cells would proliferate to produce a

closed utricular explant. Indeed, Gnedeva et al. (2017) demonstrated that utricles cultured in a low-stiffness extracellular matrix – close to our conditions – provides a conducive environment in which supporting cells can reenter their cell cycle and therefore extend the macular area. Moreover, the extracellular matrix and the N-2 supplement used in this study contain several growth factors, including EGF, bFGF and IGF-1, that should contribute to the proliferation of utricular cells and the emergence of surrounding fibroblast-like cells at 1 DIV (Zheng et al., 1997). In addition to the mechanical properties of the extracellular matrix and the use of growth factors promoting cell expansion, the maximal proliferative response of rat sensory epithelia to some growth factors has been shown to occur between birth and the 5th day post-partum (Gu et al., 2007). This time window seems to be in accordance with our observation of the development of cysts in explants from newborn rats harvested between P0 and P4. The K^+ concentration in the endolymphatic compartment (Fig. 1.B) appears to be related to the size of the vesicle. Indeed, 2-DIV cysts display a small vesicle and have a low endolymphatic K^+ concentration, whereas in 4- to 7-DIV cysts, the K^+ concentration plateaus when the vesicles reach their maximal size. This result suggests that the swelling of the cysts is triggered by the accumulation of K^+ ions, and the resulting osmotic water influx.

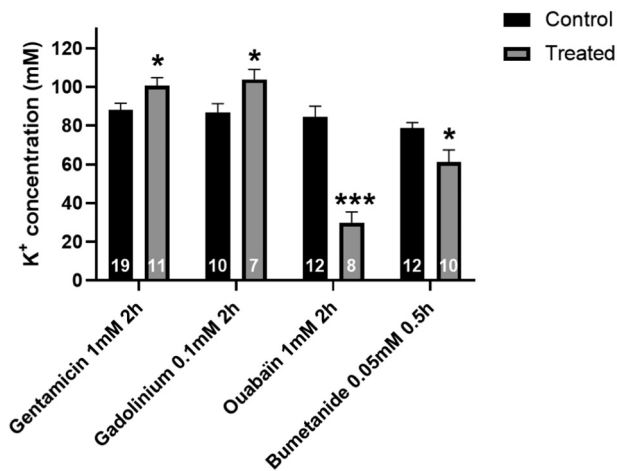


Fig. 3. Effects of inhibitors of MET channels, Na/K-ATPase and NKCC1 on endolymphatic K⁺ concentration: 7 DIV cysts obtained from P0-P4 newborn rats were treated with gentamicin (1 mM, 2 h), gadolinium (0.1 mM, 2 h), ouabain (1 mM, 2 h) or bumetanide (0.05 mM, 0.5 h). Control cysts were treated with the corresponding vehicle. Each histogram represents the mean \pm SEM; the number of samples for each group is indicated in each bar of the histogram. Student's *t*-test: **p* < .05 and ****p* < .001.

The cyst encloses an endolymph-like fluid with a high K⁺ concentration (85.8 \pm 4.8 mM at 7 DIV, Fig. 1.B), slightly below *in vivo* values (between approximately 100 and 120 mM). Endolymph is mainly produced by secretory dark cells, which transport K⁺ from perilymph to endolymph. Even though rodent dark cells appear morphologically mature at birth, the composition of endolymph only matures 6–8 days after birth (Anniko, 1980; Anniko and Nordemar, 1980). Vestibular dark cells in P0-P4 newborn rats may not yet be fully functional, which could explain why the K⁺ concentration in our model was lower than *in vivo* values. K⁺ concentrations measured in organotypic cultures of chicken embryos were also reported to be lower than *in vivo* values (Masetto et al., 2005). The K⁺ concentrations and their progression profile obtained in the current study (Fig. 1.B) are in good agreement with those reported by Bartolami et al. (2011) who described an increase in K⁺ concentration between 2 and 5 DIV, and a plateau between 5 and 8 DIV.

The endolymphatic K⁺ concentration is maintained by an active equilibrium between influx and efflux of K⁺. This equilibrium is regulated by dark and transitional cells, which secrete K⁺ into the endolymph through the action of the Na/K-ATPase pump and the NKCC1 channel expressed at their basolateral pole, and by sensory hair cells, which release K⁺ to the perilymph through transduction channels

expressed in the hair cell's stereocilia. Ouabain, a Na/K-ATPase inhibitor, and bumetanide, a NKCC1 inhibitor, both cause the K⁺ concentration to decrease, proving that the model is sensitive to the inhibition of K⁺ influx. These data are in line with those presented by Bartolami et al. (2011) using cysts obtained from P2-P3 mice: when treated with 1 mM ouabain for 1 h, the K⁺ concentration in cysts decreased by 85%; 0.05 mM bumetanide treatment for 15 min, the transient decrease was more moderate at 28%.

The involvement of sensory cells in K⁺ efflux was revealed using 2-h treatments with gentamicin and gadolinium, both of which block hair cell stretch-activated channels (Kimitsuki et al., 1996; Kroese et al., 1989). Gentamicin and gadolinium led to 14% and 20% increases in the K⁺ concentration, respectively. These percent changes are lower than those reported by Bartolami et al., (2011) with P2-P3 newborn mice cysts – at 38.6% and 56.1% increases in K⁺ after gentamicin and gadolinium treatments, respectively. The acquisition of sensory transduction during embryonic stages is well described for mouse utricles (Géléoc and Holt, 2003), but no information is available for rats. MET in rat utricle hair cells may not be fully functional during the first days after birth. In addition, the fact that utricle hair cell density in newborn rat (P1) is lower than in mice (19th gestation day) (Dechesne et al., 1986; Mbiene et al., 1984; Wubbels et al., 2002) may enhance the difference between the data reported by Bartolami et al. (2011) and the results presented here. Nevertheless, taken together the results obtained with the different pharmacological treatments confirm that all cell types involved in K⁺ cycle are functional in the present model.

To assess the vestibulotoxic potential of styrene, cysts were exposed to varying concentrations for either 2 h or 72 h. The 2-h exposure was chosen to study the pharmacological effects of styrene. Infact, several *in vivo* and *in vitro* studies showed that short exposures (30 s to 1 h) to aromatic solvents can modulate the function of *N*-methyl-D-aspartate (NMDA) and nicotinic receptors as well as Na/K-ATPase and voltage-dependent Ca²⁺ channels (VDCC) (Bale et al., 2005; Bale et al., 2002; Calderón-Guzmán et al., 2005b; Calderón-Guzmán et al., 2005a; Cruz et al., 2000; Cruz et al., 1998; Lebel and Schatz, 1990; Maguin et al., 2009; Vaalavirta and Tähti, 1995a, 1995b). The 72-h exposure-time was used to investigate the cytotoxic effects of styrene. A similar duration has previously been used to assess the effect of aromatic solvents *in vitro* on human cord blood cells (Diodovich et al., 2004), primary cortical astrocytes (Lin et al., 2002) and primary cultures of motor and sensory neurons (Kohn et al., 1995). The 72-h exposure condition was centered on the 4- to 7-DIV period, when the K⁺ concentration was stable (Fig. 1.B), so that normal cyst development would not interfere with the styrene effect.

As aromatic solvents can interact with the polystyrene walls of culture flasks, glass headspace vials were used for styrene exposure experiments (Croute et al., 2002). One major problem with experiments

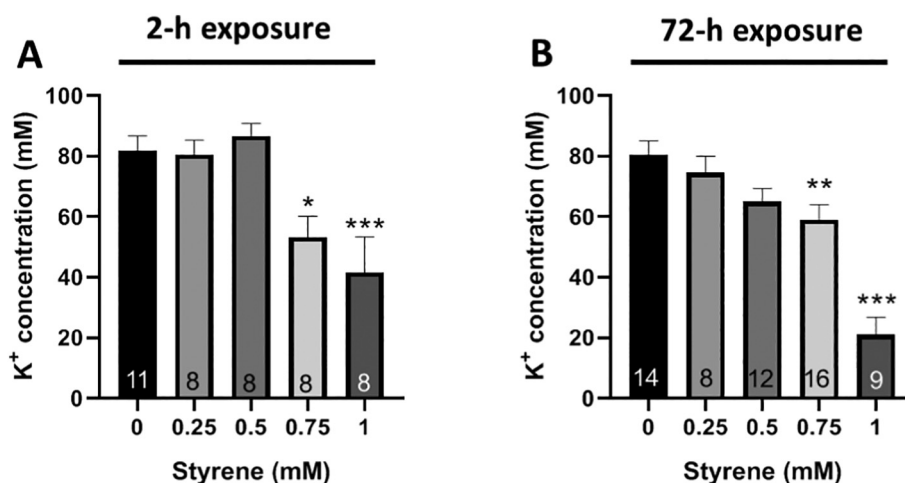


Fig. 4. Exposure to styrene decreases the endolymphatic K⁺ concentration. Cysts were obtained from P0-P4 newborn rats and measurements were performed at 7 DIV. Utricle explants were exposed to varying styrene concentrations (0.25; 0.5; 0.75 and 1 mM) for 2 h (A) or 72 h (B). Two-hour exposures were performed at 7DIV and 72-h exposures between 4 DIV and 7 DIV. Control samples were cultured in sealed vials for the corresponding exposure-time. Each histogram represents the mean \pm SEM. The number of samples is indicated in each bar of the histogram. Dunnett: **p* < .05; ***p* < .01 and ****p* < .001.

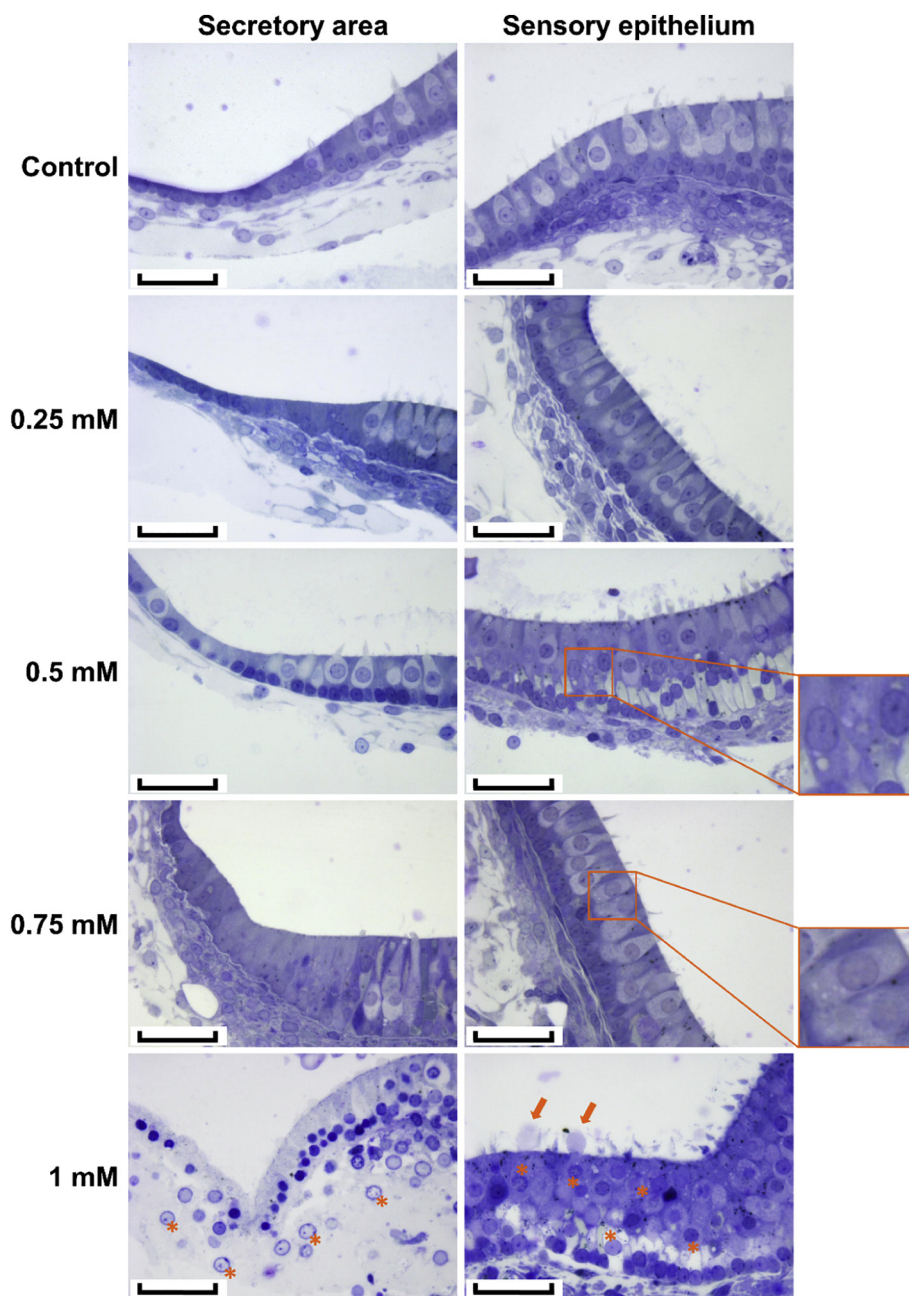


Fig. 5. Histological sections of cysts after exposure to varying styrene concentrations for 2 h. 7-DIV cysts obtained from P1-P4 newborn rats were observed under light microscopy after styrene exposure. Styrene concentrations are indicated to the left of the figure. For each condition, pictures in the left panel display part of the sensory epithelium; the right panel shows images of the secretory cell area. Cytoplasmic vacuoles were further magnified (insets). Extrusions are indicated with arrows, and condensed nuclei by asterisks. Scale bar = 40 μ M.

involving aromatic solvents is their high volatility. In unsealed containers, 25% of the solvent content is reported to evaporate within 30 min, and 90% within 4 h (Cruz et al., 1998, 2000; Rogers et al., 2004). This level of evaporation would necessarily lead to an underestimation of the toxic potency of solvents. To avoid this type of bias in our experiments, cysts were exposed to styrene in sealed vials, thus limiting evaporation and allowing a stable concentration to be maintained. This method was demonstrated to maintain more than 90% of the initial concentration of volatile organic compounds (Rogers et al., 2004).

The styrene concentrations used in this study were comprised between 0.25 and 1 mM. These concentrations were selected as they are close to styrene concentrations predicted or determined in animal blood *in vivo* after exposure. For example, the PBPK models developed by

Sarangapani et al. (2002) to predict the concentration of styrene in rodent blood indicate that after 6 h of exposure to 1200 ppm styrene, the blood concentration would be approximately 0.8 mM, and 0.25 mM after exposure to 600 ppm. Similarly, *in vivo* studies reported 0.382 mM and 0.232 mM of styrene in rat blood after inhalation exposure to 1750 ppm for 10 h and 1000 ppm for 6 h, respectively (Lataye et al., 2003; Loquet et al., 1999). Results from another study with rats exposed to styrene by oral gavage at 800 mg / kg / day indicated a blood concentration of styrene that quickly reaches a plateau at approximately 0.20 mM; this level is maintained for at least 6 h (Chen et al., 2007). In addition, the concentrations of styrene used here are of the same order of magnitude as those used in other *in vitro* studies evaluating the toxic effects of styrene in dimethyl sulfoxide (DMSO) or not (ranging from 0.1 to 10 mM for 1 to 96 h) (Diodovich et al., 2004;

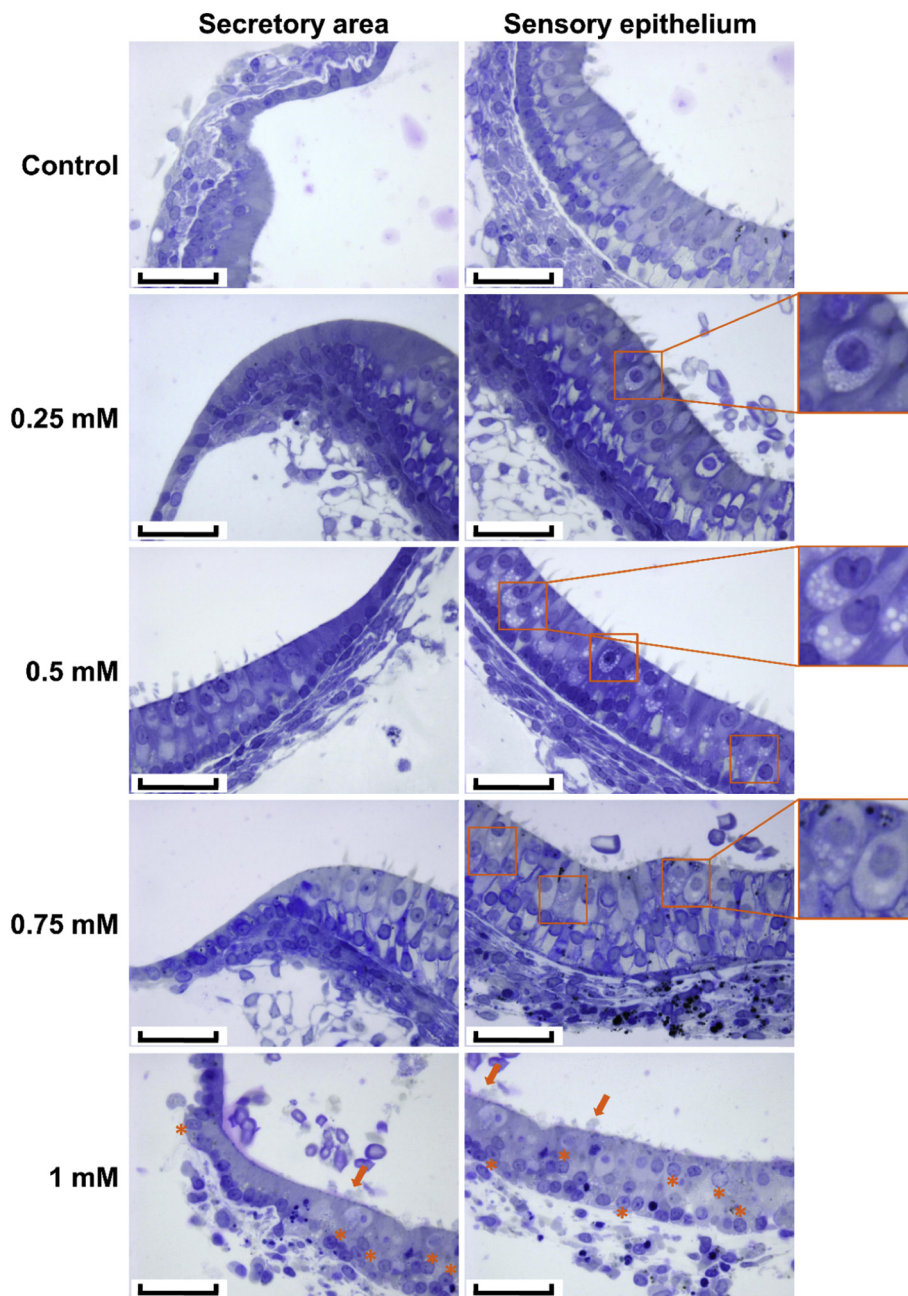


Fig. 6. Histological sections of cysts after exposure to varying styrene concentrations for 72 h. 7-DIV cysts obtained from P1–4 newborn rats were observed under light microscopy after styrene exposure. Styrene concentration is indicated to the left of the images. For each condition, the left panel displays part of the sensory epithelium; the right panel shows images of the secretory cell area. Cytoplasmic vacuoles were further magnified (insets). Extrusions are indicated with arrows, and condensed nuclei by asterisks. Scale bar = 40 μ m.

Harvilchuck et al., 2009; Harvilchuck and Carlson, 2006; Kohn et al., 1995).

Our findings from this *in vitro* study indicate that styrene decreases K^+ concentration from a solvent concentration as low as 0.75 mM after both 2- and 72-h exposure (Fig. 4). Styrene exposure induced dying cell after 2- and 72-h exposure to 1 mM and cellular suffering features from 0.5 mM after 2-h and from 0.25 mM after 72-h exposure. Indeed, histological analysis highlighted pathological features such as extrusions, low-density cytoplasm and condensed and swollen nucleus in both secretory and sensory epithelia after exposure to 1-mM styrene for 2 and 72 h. Cytoplasmic vacuoles were visible from 0.25 mM in the 72-h exposure condition. Unexpectedly, vacuoles were also observed after just 2 h exposure, but only at concentrations exceeding 0.5 mM. Based on these observations, the effects of styrene are not specific to a cell

type, and both secretory and sensory cells can be affected (Figs. 5 and 6).

The absence of cleaved caspase-3 in cysts exposed to styrene, at any concentration or duration of exposure (data not shown), indicates that styrene probably does not induce apoptotic mechanisms under the experimental conditions tested here. Indeed, the low-density cytoplasm, swollen nuclei and the absence of caspase-3 expression in cysts exposed to 1 mM of styrene for 2 h and 72 h suggest that this concentration rather induced necrosis. Diodovich et al., (2004) reported similar findings with human cord blood cells, where *in vitro* exposure to 0.8 mM of styrene for 24 h and 48 h induced necrosis and down-regulated the pro-apoptotic protein Bax. In contrast, *in vivo* studies have indicated that styrene exposure induced cochlear cell death mainly through an apoptotic pathway, and lower levels of necrosis (Chen et al.,

2007; Fetoni et al., 2016; Yang et al., 2009). This discrepancy could be explained by the fact that styrene 7,8-oxide (SO), the major metabolite of styrene, may be responsible for triggering the apoptotic pathway (Chen et al., 2007; Fetoni et al., 2016).

Although the decreased K^+ in cysts exposed to 1 mM styrene can be explained by the cytotoxic effect of the solvent, the mechanism by which K^+ decreases upon exposure to lower concentrations remains unclear. Vacuolization observed at concentrations below 1 mM may be a side effect of the action of a cytotoxic inducer, such as styrene, and cytoplasmic vacuole accumulation could be an initiating event accompanying cell death (Shubin et al., 2016). As these vacuoles appear at lower styrene concentrations than those that induce K^+ modifications, it is reasonable to conclude that K^+ concentration changes is a cause of a toxic effect of styrene and are not a simple pharmacological effect. Further studies will be needed to infer the precise toxic mechanism used by styrene.

5. Conclusion

Conventional tests to study vestibular functionality in animals and the means used to expose animals to solvent vapors are time-consuming and costly. Moreover, given the large numbers of chemicals and possible mixtures used in industry, *in vivo* testing does not appear reasonable (Bakand et al., 2005). The resulting need to develop a reliable and rapid test to determine potential vestibulotoxic effects has been taken into consideration in the present study. Cysts can be used to measure the endolymphatic K^+ concentration, which reflects the functionality of vestibular cells. Indeed, there is a probable relation between endolymph secretion anomalies and vestibular dysfunctions, such as described in Menière's disease (Farhood and Lambert, 2016; Merchant et al., 2005) as well as Jervell and Lange-Nielsen syndrome (Casimiro et al., 2001; Winbo and Rydberg, 2015). The results presented in this article show that styrene can lead to a decrease in K^+ concentration in the endolymphatic compartment associated to histopathological damages in the sensory and secretory utricular epithelia. It is therefore reasonable to suppose that this solvent may have a vestibulotoxic effect on balance. This study highlights that variations in K^+ concentration within cysts could be used as an early marker of vestibulotoxicity, and its measurement could be predictively used to distinguish between vestibulotoxic and non-vestibulotoxic compounds.

Declaration of Competing Interest

The authors declare that they have no known competing financial interests or personal relationships that could have appeared to influence the work reported in this paper.

Acknowledgments

The authors would like to thank Marie-Joseph Décret and Laurine Douteau for their help with animal handling and husbandry, and Aurélie Remy for statistical analysis.

References

Anniko, M., 1980. Embryologic development in vivo and in vitro of the dark cell region of the mammalian crista ampullaris. *Acta Otolaryngol.* 90, 106–114. <https://doi.org/10.3109/00016488009131705>.

Anniko, M., Nordemar, H., 1980. Embryogenesis of the inner ear. IV. Post-natal maturation of the secretory epithelia of the inner ear in correlation with the elemental composition in the endolymphatic space. *Arch Otorhinolaryngol* 229, 281–288.

Bakand, S., Winder, C., Khalil, C., Hayes, A., 2005. Toxicity assessment of industrial chemicals and airborne contaminants: transition from in vivo to in vitro test methods: a review. *Inhal. Toxicol.* 17, 775–787. <https://doi.org/10.1080/08958370500225240>.

Bale, A.S., Smothers, C.T., Woodward, J.J., 2002. Inhibition of neuronal nicotinic acetylcholine receptors by the abused solvent, toluene. *Br. J. Pharmacol.* 137, 375–383. <https://doi.org/10.1038/sj.bjp.0704874>.

Bale, A.S., Meacham, C.A., Benignus, V.A., Bushnell, P.J., Shafer, T.J., 2005. Volatile organic compounds inhibit human and rat neuronal nicotinic acetylcholine receptors expressed in *Xenopus* oocytes. *Toxicol. Appl. Pharmacol.* 205, 77–88. <https://doi.org/10.1016/j.taap.2004.09.011>.

Bartolami, S., Gaboyard, S., Quentin, J., Travo, C., Cavalier, M., Barhanin, J., Chabbert, C., 2011. Critical roles of transitional cells and Na/K-ATPase in the formation of vestibular Endolymph. *J. Neurosci.* 31, 16541–16549. <https://doi.org/10.1523/JNEUROSCI.2430-11.2011>.

Bergamaschi, E., Smargiassi, A., Mutti, A., Cavazzini, S., Vettori, M.V., Alinovi, R., Franchini, I., Mergler, D., 1997. Peripheral markers of catecholaminergic dysfunction and symptoms of neurotoxicity among styrene-exposed workers. *Int. Arch. Occup. Environ. Health* 69, 209–214.

Calabrese, G., Martini, A., Sessa, G., Cellini, M., Bartolucci, G.B., Marcuzzo, G., De Rosa, E., 1996. Otoneurological study in workers exposed to styrene in the fiberglass industry. *Int. Arch. Occup. Environ. Health* 68, 219–223.

Calderón-Guzmán, D., Espitia-Vázquez, I., López-Domínguez, A., Hernández-García, E., Huerta-Gertrudis, B., Coballase-Urritia, E., Juárez-Olgún, H., García-Fernández, B., 2005a. Effect of toluene and nutritional status on serotonin, lipid peroxidation levels and NA⁺/K⁺-ATPase in adult rat brain. *Neurochem. Res.* 30, 619–624. <https://doi.org/10.1007/s11064-005-2749-2>.

Calderón-Guzmán, D., Hernández-Islas, J.L., Espitia Vázquez, I.R., Barragán-Mejía, G., Hernández-García, E., Del Angel, D.S., Juárez-Olgún, H., 2005b. Effect of toluene and cresols on Na⁺/K⁺-ATPase, and serotonin in rat brain. *Regul. Toxicol. Pharmacol.* 41, 1–5. <https://doi.org/10.1016/j.yrtph.2004.09.005>.

Callejo, A., Durochat, A., Bressieux, S., Saleur, A., Chabbert, C., Domènech Juan, I., Llorens, J., Gaboyard-Niay, S., 2017. Dose-dependent cochlear and vestibular toxicity of trans-tympanic cisplatin in the rat. *Neurotoxicology* 60, 1–9. <https://doi.org/10.1016/j.neuro.2017.02.007>.

Campo, P., Loquet, G., Blachère, V., Roue, M., 1999. Toluene and styrene intoxication route in the rat cochlea. *Neurotoxicol. Teratol.* 21, 427–434.

Campo, P., Lataye, R., Loquet, G., Bonnet, P., 2001. Styrene-induced hearing loss: a membrane insult. *Hear. Res.* 154, 170–180.

Casimiro, M.C., Knollmann, B.C., Ebert, S.N., Vary, J.C., Greene, A.E., Franz, M.R., Grinberg, A., Huang, S.P., Pfeifer, K., 2001. Targeted disruption of the *Kcqn1* gene produces a mouse model of Jervell and Lange-Nielsen syndrome. *Proc. Natl. Acad. Sci. U. S. A.* 98, 2526–2531. <https://doi.org/10.1073/pnas.041398998>.

Chen, G.-D., Chi, L.-H., Kostyniak, P.J., Henderson, D., 2007. Styrene induced alterations in biomarkers of exposure and effects in the cochlea: mechanisms of hearing loss. *Toxicol. Sci.* 98, 167–177. <https://doi.org/10.1093/toxsci/kfm078>.

Cioman, R.R., 2009. Stria vascularis and vestibular dark cells: characterisation of main structures responsible for inner-ear homeostasis, and their pathophysiological relations. *J. Laryngol. Otol.* 123, 151. <https://doi.org/10.1017/S0022215108002624>.

Crout, F., Poinot, J., Gaubin, Y., Beau, B., Simon, V., Murat, J.C., Soleilhavoup, J.P., 2002. Volatile organic compounds cytotoxicity and expression of HSP72, HSP90 and GRP78 stress proteins in cultured human cells. *Biochim. Biophys. Acta* 1591, 147–155. [https://doi.org/10.1016/s0167-4889\(02\)00271-9](https://doi.org/10.1016/s0167-4889(02)00271-9).

Cruz, S.L., Mirshahi, T., Thomas, B., Balster, R.L., Woodward, J.J., 1998. Effects of the abused solvent toluene on recombinant N-methyl-D-aspartate and non-N-methyl-D-aspartate receptors expressed in *Xenopus* oocytes. *J. Pharmacol. Exp. Ther.* 286, 334–340.

Cruz, S.L., Balster, R.L., Woodward, J.J., 2000. Effects of volatile solvents on recombinant N-methyl-D-aspartate receptors expressed in *Xenopus* oocytes. *Br. J. Pharmacol.* 131, 1303–1308. <https://doi.org/10.1038/sj.bjp.0703666>.

Dechesne, C., Mbiene, J.P., Sans, A., 1986. Postnatal development of vestibular receptor surfaces in the rat. *Acta Otolaryngol.* 101, 11–18. <https://doi.org/10.3109/00016488609108602>.

Diodovich, C., Bianchi, M.G., Bowe, G., Acquati, F., Taramelli, R., Parent-Massin, D., Gribaldo, L., 2004. Response of human cord blood cells to styrene exposure: evaluation of its effects on apoptosis and gene expression by genomic technology. *Toxicology* 200, 145–157. <https://doi.org/10.1016/j.tox.2004.03.021>.

Farhood, Z., Lambert, P.R., 2016. The physiologic role of corticosteroids in Ménière's disease. *Am. J. Otolaryngol.* 37, 455–458. <https://doi.org/10.1016/j.amjoto.2016.04.004>.

Fetoni, A.R., Rolesi, R., Paciello, F., Eramo, S.L.M., Grassi, C., Troiani, D., Paludetti, G., 2016. Styrene enhances the noise induced oxidative stress in the cochlea and affects differently mechanosensory and supporting cells. *Free Radic. Biol. Med.* 101, 211–225. <https://doi.org/10.1016/j.freeradbiomed.2016.10.014>.

Gaboyard, S., Chabbert, C., Travo, C., Bancel, F., Lehouelleur, J., Yamauchi, D., Marcus, D.C., Sans, A., 2005. Three-dimensional culture of newborn rat utricle using an extracellular matrix promotes formation of a cyst. *Neuroscience* 133, 253–265. <https://doi.org/10.1016/j.neuroscience.2005.02.011>.

Gagnaire, F., Langlais, C., 2005. Relative ototoxicity of 21 aromatic solvents. *Arch. Toxicol.* 79, 346–354. <https://doi.org/10.1007/s00204-004-0636-2>.

Gans, R.E., Rauterkuus, G., Research Associate 1, 2019. Vestibular toxicity: causes, evaluation protocols, intervention, and management. *Semin. Hear.* 40, 144–153. <https://doi.org/10.1055/s-0039-1684043>.

Géléoc, G.S.G., Holt, J.R., 2003. Developmental acquisition of sensory transduction in hair cells of the mouse inner ear. *Nat. Neurosci.* 6, 1019–1020. <https://doi.org/10.1038/nn1120>.

Gnedeva, K., Jacobo, A., Salvi, J.D., Petelski, A.A., Hudspeth, A.J., 2017. Elastic force restricts growth of the murine utricle. *Elife* 6. <https://doi.org/10.7554/eLife.25681>.

Gu, R., Montcouquiol, M., Marchionni, M., Corwin, J.T., 2007. Proliferative responses to growth factors decline rapidly during postnatal maturation of mammalian hair cell epithelia. *Eur. J. Neurosci.* 25, 1363–1372. <https://doi.org/10.1111/j.1460-9568.2007.05414.x>.

Harvilchuck, J.A., Carlson, G.P., 2006. Comparison of styrene and its metabolites styrene

- oxide and 4-vinylphenol on cytotoxicity and glutathione depletion in Clara cells of mice and rats. *Toxicology* 227, 165–172. <https://doi.org/10.1016/j.tox.2006.08.001>.
- Harvilchuck, J.A., Pu, X., Klauing, J.E., Carlson, G.P., 2009. Indicators of oxidative stress and apoptosis in mouse whole lung and Clara cells following exposure to styrene and its metabolites. *Toxicology* 264, 171–178. <https://doi.org/10.1016/j.tox.2009.08.001>.
- Hibino, H., Kurachi, Y., 2006. Molecular and physiological bases of the K^+ circulation in the mammalian inner ear. *Physiology* 21, 336–345. <https://doi.org/10.1152/physiol.00023.2006>.
- Hibino, H., Nin, F., Tsuzuki, C., Kurachi, Y., 2010. How is the highly positive endocochlear potential formed? The specific architecture of the stria vascularis and the roles of the ion-transport apparatus. *Pflügers Arch.* 459, 521–533. <https://doi.org/10.1007/s00424-009-0754-z>.
- Hoet, P., Lison, D., 2008. Ototoxicity of toluene and styrene: state of current knowledge. *Crit. Rev. Toxicol.* 38, 127–170. <https://doi.org/10.1080/10408440701845443>.
- Johnson, A.-C., 2007. Relationship between styrene exposure and hearing loss: review of human studies. *Int. J. Occup. Med. Environ. Health* 20, 315–325. <https://doi.org/10.2478/s10001-007-0040-2>.
- Kim, H.J., Lee, J.O., Koo, J.W., Kim, J.-S., Ban, J., 2013. Gentamicin-induced bilateral vestibulopathy in rabbits: vestibular dysfunction and histopathology. *Laryngoscope* 123, E51–E58. <https://doi.org/10.1002/lary.24106>.
- Kimitsuki, T., Nakagawa, T., Hisashi, K., Komune, S., Komiya, S., 1996. Gadolinium blocks mechano-electric transducer current in chick cochlear hair cells. *Hear. Res.* 101, 75–80. [https://doi.org/10.1016/S0378-5955\(96\)00134-7](https://doi.org/10.1016/S0378-5955(96)00134-7).
- Kishi, R., Tozaki, S., Gong, Y.Y., 2000. Impairment of neurobehavioral function and color vision loss among workers exposed to low concentration of styrene—a review of literatures. *Ind. Health* 38, 120–126.
- Kohn, J., Minotti, S., Durham, H., 1995. Assessment of the neurotoxicity of styrene, styrene oxide, and styrene glycol in primary cultures of motor and sensory neurons. *Toxicol. Lett.* 75, 29–37. [https://doi.org/10.1016/0378-4274\(94\)03153-x](https://doi.org/10.1016/0378-4274(94)03153-x).
- Kroese, A.B., Das, A., Hudspeth, A.J., 1989. Blockage of the transduction channels of hair cells in the bullfrog's sacculus by aminoglycoside antibiotics. *Hear. Res.* 37, 203–217.
- Larsby, B., Tham, R., Odqvist, L.M., Hydén, D., Bunnfors, I., Aschan, G., 1978. Exposure of rabbits to styrene. Electronystagmographic findings correlated to the styrene level in blood and cerebrospinal fluid. *Scand. J. Work Environ. Health* 4, 60–65.
- Lataye, R., Campo, P., Barthelemy, C., Loquet, G., Bonnet, P., 2001. Cochlear pathology induced by styrene. *Neurotoxicol. Teratol.* 23, 71–79.
- Lataye, R., Campo, P., Pouyatos, B., Cossec, B., Blachère, V., Morel, G., 2003. Solvent ototoxicity in the rat and Guinea pig. *Neurotoxicol. Teratol.* 25, 39–50.
- Lebel, C.P., Schatz, R.A., 1990. Altered synaptosomal phospholipid metabolism after toluene: possible relationship with membrane fluidity, Na^+ , K^+ -adenosine triphosphatase and phospholipid methylation. *J. Pharmacol. Exp. Ther.* 253, 1189–1197.
- Lin, H.J., Shaffer, K.M., Chang, Y.H., Barker, J.L., Pancrazio, J.J., Stenger, D.A., Ma, W., 2002. Acute exposure of toluene transiently potentiates p42/44 mitogen-activated protein kinase (MAPK) activity in cultured rat cortical astrocytes. *Neurosci. Lett.* 332, 103–106. [https://doi.org/10.1016/S0304-3940\(02\)00930-8](https://doi.org/10.1016/S0304-3940(02)00930-8).
- Llorens, J., Demêmes, D., Sans, A., 1993. The behavioral syndrome caused by 3,3'-iminodipropionitrile and related nitriles in the rat is associated with degeneration of the vestibular sensory hair cells. *Toxicol. Appl. Pharmacol.* 123, 199–210. <https://doi.org/10.1006/taap.1993.1238>.
- Loquet, G., Campo, P., Lataye, R., 1999. Comparison of toluene-induced and styrene-induced hearing losses. *Neurotoxicol. Teratol.* 21, 689–697.
- Maguin, K., Campo, P., Parietti-Winkler, C., 2009. Toluene can perturb the neuronal voltage-dependent Ca^{2+} channels involved in the middle-ear reflex. *Toxicol. Sci.* 107, 473–481. <https://doi.org/10.1093/toxsci/kfn242>.
- Masetto, S., Zucca, G., Bottà, L., Valli, P., 2005. Endolymphatic potassium of the chicken vestibule during embryonic development. *Int. J. Dev. Neurosci.* 23, 439–448. <https://doi.org/10.1016/j.ijdevneu.2005.05.002>.
- Mbiene, J.P., Favre, D., Sans, A., 1984. The pattern of ciliary development in fetal mouse vestibular receptors. A qualitative and quantitative SEM study. *Anat. Embryol.* 170, 229–238. <https://doi.org/10.1007/bf00318726>.
- Merchant, S.N., Adams, J.C., Nadol, J.B., 2005. Pathophysiology of Meniere's syndrome: are symptoms caused by endolymphatic hydrops? *Otol. Neurotol.* 26, 74–81.
- Meredith, F.L., Rennie, K.J., 2016. Channeling your inner ear potassium: K^+ channels in vestibular hair cells. *Hear. Res.* 338, 40–51. <https://doi.org/10.1016/j.heares.2016.01.015>.
- Miller, R.R., Newhook, R., Poole, A., 1994. Styrene production, use, and human exposure. *Crit. Rev. Toxicol.* 24, S1–S10. <https://doi.org/10.3109/10408449409020137>.
- Möller, C., Odqvist, L., Larsby, B., Tham, R., Ledin, T., Bergholtz, L., 1990. Otoneurological findings in workers exposed to styrene. *Scand. J. Work Environ. Health* 16, 189–194.
- Nicolas, M., Demêmes, D., Martin, A., Kupersmidt, S., Barhanin, J., 2001. KCNQ1/KCNE1 potassium channels in mammalian vestibular dark cells. *Hear. Res.* 153, 132–145. [https://doi.org/10.1016/S0378-5955\(00\)00268-9](https://doi.org/10.1016/S0378-5955(00)00268-9).
- Nicolas, M.-T., Lesage, F., Reyes, R., Barhanin, J., Demêmes, D., 2004. Localization of TREK-1, a two-pore-domain K^+ channel in the peripheral vestibular system of mouse and rat. *Brain Res.* 1017, 46–52. <https://doi.org/10.1016/j.brainres.2004.05.012>.
- Niklasson, M., Tham, R., Larsby, B., Eriksson, B., 1993. Effects of toluene, styrene, trichloroethylene, and trichloroethane on the vestibulo-and opto-oculo motor system in rats. *Neurotoxicol. Teratol.* 15, 327–334.
- Pleban, F.T., Oketope, O., Shrestha, L., 2017. Occupational styrene exposure on auditory function among adults: a systematic review of selected workers. *Saf. Health Work* 8, 329–336. <https://doi.org/10.1016/j.shaw.2017.01.002>.
- Popper, P., Winkler, J., Erbe, C.B., Lerch-Gaggl, A., Siebeneich, W., Wackym, P.A., 2008. Distribution of two-pore-domain potassium channels in the adult rat vestibular periphery. *Hear. Res.* 246, 1–8. <https://doi.org/10.1016/j.heares.2008.09.004>.
- Rogers, J.V., Siegel, G.L., Pollard, D.L., Rooney, A.D., McDougal, J.N., 2004. The cytotoxicity of volatile JP-8 jet fuel components in keratinocytes. *Toxicology* 197, 113–121. <https://doi.org/10.1016/j.tox.2003.12.011>.
- Sarangapani, R., Teeguarden, J.G., Cruzan, G., Clewell, H.J., Andersen, M.E., 2002. Physiologically based pharmacokinetic modeling of styrene and styrene oxide respiratory-tract dosimetry in rodents and humans. *Inhal. Toxicol.* 14, 789–834. <https://doi.org/10.1080/08958370290084647>.
- Shubin, A.V., Demidyuk, I.V., Komissarov, A.A., Rafieva, L.M., Kostrov, S.V., 2016. Cytoplasmic vacuolization in cell death and survival. *Oncotarget* 7, 55863–55889. <https://doi.org/10.18632/oncotarget.10150>.
- Spicer, S.S., Schulte, B.A., 1998. Evidence for a medial K^+ recycling pathway from inner hair cells. *Hear. Res.* 118, 1–12.
- Toppila, E., Forsman, P., Pyykkö, I., Starck, J., Tossavainen, T., Uitti, J., Oksa, P., 2006. Effect of styrene on postural stability among reinforced plastic boat plant workers in Finland. *J. Occup. Environ. Med.* 48, 175–180. <https://doi.org/10.1097/01.jom.0000199510.80882.7b>.
- Vaalavirta, L., Tähti, H., 1995a. Astrocyte membrane Na^+ , K^+ -ATPase and $mg(2^+)$ -ATPase as targets of organic solvent impact. *Life Sci.* 57, 2223–2230. [https://doi.org/10.1016/0024-3205\(95\)02214-4](https://doi.org/10.1016/0024-3205(95)02214-4).
- Vaalavirta, L., Tähti, H., 1995b. Effects of selected organic solvents on the astrocyte membrane ATPase in vitro. *Clin. Exp. Pharmacol. Physiol.* 22, 293–294. <https://doi.org/10.1111/j.1440-1681.1995.tb01999.x>.
- Vouiriou, A., Hannhart, B., Gauchard, G.C., Barot, A., Ledin, T., Mur, J.-M., Perrin, P.P., 2005. Long-term exposure to solvents impairs vigilance and postural control in serigraphy workers. *Int. Arch. Occup. Environ. Health* 78, 510–515. <https://doi.org/10.1007/s00420-005-0609-7>.
- Winbo, A., Rydberg, A., 2015. Vestibular dysfunction is a clinical feature of the Jervell and Lange-Nielsen syndrome. *Scand. Cardiovasc. J.* 49, 7–13. <https://doi.org/10.3109/14017431.2014.988172>.
- Wubbels, R.J., de Jong, H., van Marle, J., 2002. Morphometric analysis of the vestibular sensory epithelia of young adult rat. *Vestib. Res.* 12, 145–154.
- Yang, W.P., Hu, B.H., Chen, G.D., Bielefeld, E.C., Henderson, D., 2009. Protective effect of N-acetyl-L-cysteine (L-NAC) against styrene-induced cochlear injuries. *Acta Otolaryngol.* 129, 1036–1043. <https://doi.org/10.1080/00016480802566261>.
- Zheng, J.L., Helbig, C., Gao, W.Q., 1997. Induction of cell proliferation by fibroblast and insulin-like growth factors in pure rat inner ear epithelial cell cultures. *J. Neurosci.* 17, 216–226.